How to Develop Future Weather Data for Building Energy Modeling

Zhaoyun ZENG[1]*, Ji-Hyun (Jeannie) KIM[1], Ralph T. MUEHLEISEN[1]

[1]Argonne National Laboratory, Energy Systems and Infrastructure Analysis Division,
Lemont, Illinois, USA
zengz@anl.gov

* Corresponding Author

ABSTRACT

Future weather data is essential for assessing the impacts of climate change on building performance. However, the building energy modeling community has been struggling with a lack of high-quality future weather datasets specifically designed for this purpose, leading to widespread misprocessing and misuse of the data. To address this issue, we provide an overview of the methodology used to create future weather data, including aspects such as emissions scenarios, general circulation models, downscaling techniques, and the various types of future weather data. Additionally, we introduce a dynamically downscaled future weather dataset developed by Argonne National Laboratory and showcase its superior qualities through a case study.

1. INTRODUCTION

Climate change is one of the most significant challenges of our time, involving both a gradual rise in global mean temperature and a notable increase in the frequency, intensity, and duration of extreme weather events like heat waves and rainstorms (Coumou & Rahmstorf, 2012; Meehl & Tebaldi, 2004; Van Aalst, 2006). To accommodate these changes, building design must incorporate concepts of adaptability to a wide range of weather conditions and resilience to future extreme weather events.

To assess the impacts of climate change on building performance, future weather data can be used in building energy modeling (BEM). While future weather data has long been available for fields such as agriculture and hydrology, its creation for BEM has been lacking due to two unique characteristics: short time scales and a broad range of impactful variables. Because buildings are highly sensitive to short-term weather fluctuations, weather data for buildings should be on hourly or sub-hourly time scales (Herrera et al., 2017a). Furthermore, building performance is affected by a broad scope of weather variables, including dry-bulb temperature, wet-bulb temperature, solar irradiance, sky temperature, wind speed and direction, and atmospheric pressure, among others (Crawley & Barnaby, 2019). The development of future weather data for use in BEM is a significant industry need. This paper presents an overview of the methodology used to create future weather data for buildings and provides an example of its application.

1.1 Emissions Scenarios

Climate change is influenced by a multitude of uncertain factors, including technological advancements, economic growth, and societal decisions on future development. To standardize the assessment of climate change impacts, the Intergovernmental Panel on Climate Change (IPCC) and the broader climate research community have developed various scenarios to capture the range of possible future development trajectories (O'Neill et al., 2020). Each scenario offers a plausible description of how socioeconomic, technological and environmental conditions, emissions of greenhouse gases and aerosols, and hence the climate might evolve over the next few decades (Moss et al., 2010).

Currently, two main generations of emissions scenarios are in widespread use. The first, known as the Representative Concentration Pathways (RCPs), was released in 2009 (Moss et al., 2010). The RCPs comprise four emissions scenarios selected to represent the full range of stabilization, mitigation, and reference emissions scenarios available in the literature. These scenarios are named according to the expected radiative forcing level for 2100: RCP2.6 (a low forcing, mitigation scenario), RCP4.5 and RCP6 (medium stabilization scenarios), and RCP8.5 (a high baseline emissions scenario) (van Vuuren et al., 2011).

The second generation, the Shared Socioeconomic Pathways (SSPs), includes five socioeconomic pathways that project future developments in population, education, urbanization, and economic growth. SSP1 represents a sustainable pathway with low challenges to mitigation and adaptation, SSP2 is a "middle-of-the-road" pathway with medium challenges to mitigation and adaptation, SSP3 focuses on regional rivalry with high challenges to mitigation and adaptation, SSP4 emphasizes inequality with high challenges to mitigation but low challenges to adaptation, and SSP5 envisions continued fossil-fueled development with high challenges to mitigation and low challenges to adaptation (Riahi et al., 2017). The SSPs can be combined with radiative forcing levels to form integrated scenarios (van Vuuren et al., 2014). The Sixth Assessment Report (AR6) of the IPCC adopted a core set of five illustrative scenarios based on the SSPs (SSP1-1.9, SSP1-2.6, SSP2-4.5, SSP3-7.0, and SSP5-8.5), which cover a broader range of greenhouse gas and air pollutant futures than the RCPs (Intergovernmental Panel on Climate Change, 2021).

1.2 General Circulation Models

Data from emissions scenarios, including time series of greenhouse gas and air pollutant emissions and concentrations, as well as land use and land cover changes, serve as input for general circulation models (GCMs). These models are the primary tools for projecting the long-term evolution of the climate system (Intergovernmental Panel on Climate Change, 2021). GCMs employ a set of mathematical equations, discretized on three-dimensional grids, to simulate the movement of mass and energy in the atmosphere and oceans. While some equations are derived from fundamental physical laws, many physical processes are estimated using empirical relationships from observations, known as parameterizations (Intergovernmental Panel on Climate Change, 2021). State-of-the-art GCMs, also known as earth system models, comprise separate modules representing the atmosphere, ocean, cryosphere, land use, biosphere, and the carbon and sulfur cycles (Flato, 2011).

The spatial resolution of GCMs, constrained by the computational capabilities of modern supercomputers, typically ranges from 100 to 200 km (Hannah, 2022). This coarse resolution significantly restricts their ability to simulate local phenomena and generate the local-scale climate change information required by BEM (Giorgi, 2008). Additionally, GCM outputs are generally stored on a daily or monthly basis to reduce storage requirements (Meehl et al., 2007; Taylor et al., 2012). Consequently, to make GCM outputs suitable for BEM, both spatial and temporal downscaling are necessary.

1.3 Downscaling

Downscaling techniques are categorized into two main types: dynamical downscaling and statistical downscaling. Dynamical downscaling employs physics-based climate models with higher spatial resolutions (typically 10–30 km), known as regional climate models (RCMs), to refine GCM outputs. Unlike GCMs, which cover the entire globe, RCMs focus on specific regions (Feser et al., 2011; Giorgi & Bates, 1989; Giorgi & Mearns, 1991; Yang, 2015) and use GCM outputs as their boundary conditions (Feser et al., 2011). This increased resolution allows RCMs to better represent key drivers of regional climate, such as mountain ranges and urban effects, and to capture local atmospheric phenomena like orographic precipitation more accurately (Ekström et al., 2015). However, the substantial computational demands of running RCMs significantly limit their application in BEM (Wang et al., 2021).

The advantages of dynamical downscaling are illustrated in Figure 1, where GCMs, with their coarse grids, simplify the terrain of Western North America into a single plateau and nearly erase the Appalachian Mountains. In contrast, an RCM with a 12 km horizontal resolution clearly distinguishes between various mountain ranges, basins, and valleys.

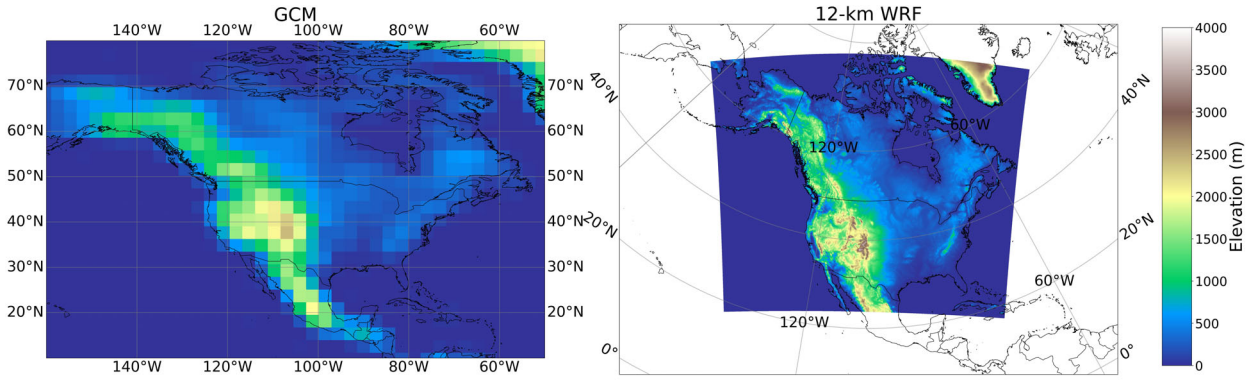

Figure 1: Representation of North America terrain in a GCM and the 12-km WRF simulation

Statistical downscaling involves techniques that use empirical relationships between local-scale variables and large-scale atmospheric variables. This approach is significantly less resource-intensive than dynamical downscaling but comes with challenges, such as dependence on the quality of training data and difficulty in accurately capturing the correlations between different variables and their spatial dynamics (Giorgi, 2008). Additionally, each statistical downscaling technique has its own specific limitations.

In BEM, the most widely used statistical downscaling methods are morphing and stochastic weather generators (SWGs). The morphing technique applies low-resolution climate change signals to high-resolution baseline weather data by shifting, stretching, or combining these adjustments (Belcher et al., 2005). The baseline weather data typically comes from observations, while the climate change signals are derived from GCMs or RCMs (Belcher et al., 2005; New et al., 2007; Vidal & Wade, 2008). The simplicity of the morphing technique has made it the most popular downscaling method in BEM. However, its ability to accurately represent the intensity and frequency of future extreme weather events is limited (Jentsch et al., 2008).

SWGs are statistical models designed to efficiently simulate random sequences of weather variables (typically on a daily basis) that closely resemble the characteristics of the observed weather data (Wilks & Wilby, 1999). Parametric SWGs use stochastic models, such as Markov chains, to classify days as wet or dry and then estimate other weather variables based on this classification (Herrera et al., 2017b; Wilks & Wilby, 1999). In contrast, non-parametric SWGs directly resample weather data from historical records using algorithms like k-nearest neighbors (Herrera et al., 2017b; Wilks & Wilby, 1999). A key advantage of SWGs is their ability to generate weather series of arbitrary length, which is valuable for risk and uncertainty analysis (Kyselý & Dubrovský, 2005). However, their standard operation on a daily timestep limits their ability to generate weather data at an hourly interval (Wilks & Wilby, 1999). To address this, methods such as extracting prevailing patterns from historical records are employed (Eames et al., 2011; Watkins et al., 2011), although these approaches constrain SWGs' capability to accurately represent the diurnal variations of weather variables.

1.4 Categories of Future Weather Data

Future weather data can be divided into three main categories: chronological weather data, typical weather data, and extreme weather data. Chronological weather data refers to projected weather data for consecutive calendar years in the future and serves as the raw material for generating both typical and extreme weather data. Unlike historical weather data, chronological weather data should not be attributed to specific future years, as the goal of climate projection is to characterize the statistical properties of future weather over a general time period rather than predict actual future weather conditions (Intergovernmental Panel on Climate Change, 2021).

Typical weather data is a synthetic year composed of 12 representative calendar months that can reflect the long-term average climate conditions of a location. It can be created using two approaches. The first approach involves directly morphing present Typical Meteorological Years (TMYs) using climate change projections from GCMs (Belcher et al., 2005). The second approach uses the Sandia method, which is the method used to create TMYs, to select representative months from future chronological weather data and concatenate them into a typical year (Bass, Brett et al., 2022; Qian et al., 2023).

Extreme weather data represents various types of extreme weather conditions in the future. For instance, an Extreme Warm Year (EWY) consists of 12 extreme warm months, while an Extreme Cold Year (ECY) contains 12 extreme cold months (Nik, 2016). Another example is the Design Summer Year (DSY) adopted in the U.K., which is defined as the year with a summer overheating return period equal to seven years (Eames, 2016). Besides complete years, it is also beneficial to use specific periods of weather data that contain certain extreme weather events in BEM. This method not only reduces computational cost but also enhances flexibility in selecting desired weather conditions (Baniassadi et al., 2018; Villa et al., 2023; Zeng et al., 2022).

2. ARGONNE FUTURE WEATHER DATASET

As part of a nationwide effort supported by the U.S. Department of Energy to promote the integration of future weather data into energy conservation codes and building design practices, Argonne National Laboratory developed a dynamically downscaled future weather dataset. This dataset is based on projections from the Community Climate System Model version 4 (CCSM4), a GCM with a horizontal resolution of 0.9° × 1.25° (latitude × longitude) (Gent et al., 2011). The output of CCSM4 is then downscaled by the Weather Research and Forecasting (WRF) model version 3.3.1, an RCM with a horizontal resolution of 12 km (Powers et al., 2017). This high spatial resolution allows the dataset to realistically capture local-scale climate features, such as the urban heat island effect.

The domain of the WRF simulations, illustrated in Figure 1, covers most of the North America. This dataset was developed within the RCP framework, as the SSPs had not been released at the onset of this project. It encompasses two emissions scenarios: RCP4.5, representing a medium scenario, and RCP8.5, representing a worst-case scenario. The dataset provides chronological weather data for two future 10-year periods: the mid-21st century (2045–2054, referred to as the 2050s) and the late 21st century (2085–2094, referred to as the 2090s). Given the significant interannual variations in climate (Intergovernmental Panel on Climate Change, 2021), it is strongly recommended to use the full 10-year span for evaluating building performance in future periods rather than selecting a single arbitrary year. This approach helps mitigate biases introduced by interannual variations.

Since the WRF model output is stored with a temporal resolution of 3 hours, we developed a suite of methods combining physics-based modeling with statistical interpolation to downscale it to an hourly interval. The methods for deriving weather variables in the Argonne Future Weather Dataset are outlined in Table 1. Using these methods, the physical coherence between different weather variables is preserved.

Table 1: Methods for deriving weather variables in the Argonne Future Weather Dataset

	Weather variable	Unit	Derivation method
1	Dry-Bulb Temperature	°C	Interpolated from WRF output using cubic spline
2	Dew Point Temperature	°C	
3	Relative Humidity	%	
4	Atmospheric Pressure	Pa	
5	Horizontal Infrared Radiation Intensity from Sky	W/m^2	
6	Wind Speed	m/s	
7	Wind Direction	°	
8	Global Horizontal Irradiation	W/m^2	Derived using WRF output, the Ineichen model (Ineichen, 2008), and linear interpolation
9	Direct Normal Irradiation	W/m^2	Derived using WRF output, the Ineichen model (Ineichen, 2008), the DRINT model (Perez et al., 1992), and linear interpolation
10	Diffuse Horizontal Irradiation	W/m^2	
11	Sky Cover	in tenths	Derived using WRF output, the Clark and Allen model (Clark & Allen, 1978), the Walton model (Walton, 1983), and cubic spline interpolation
12	Albedo	-	Copied from the monthly average values of the nearest TMY3 site
13	Liquid Precipitation Depth	mm	Linearly interpolated from WRF output

In the initial release of this dataset, we provide future weather data for the centroid of each Public Use Microdata Area (PUMA). PUMAs are non-overlapping, statistical geographic areas that divide each state or equivalent entity into regions containing no fewer than 100,000 people each. There are 2,378 PUMAs in total, covering the entire U.S. (US Census Bureau, 2022). The weather files are available in EPW format and can be freely accessed at https://data.openei.org/submissions/5974.

3. CASE STUDY

In this section, we present a case study to demonstrate the Argonne Future Weather Dataset's capability in capturing urban microclimates. This study evaluates the performance of a prototype single-family detached house with a conditioned area of 221 m^2 at the centroids of 11 PUMAs (denoted as P1–P11) in the Chicago Metropolitan Area under RCP8.5 (Pacific Northwest National Laboratory, 2013). The locations of these centroids are shown in Figure 2. In addition to future weather data, TMY3 weather data from O'Hare International Airport and reanalysis weather data for the period from 2001 to 2021 (denoted as 2010s), obtained from the National Aeronautics and Space Administration (NASA) Prediction of Worldwide Energy Resources (POWER) website, are used as the baseline (NASA Langley Research Center, 2023).

Figure 2: Locations of the selected PUMA centroids

Figure 3 presents the probability density functions for summer temperatures (June, July, and August) at four selected locations. Among these locations, P1 is situated in a rural setting, while P5 is located in a suburban area. P6 and P8, both positioned in urban areas, differ in that the latter is on the lakeshore, whereas the former is further inland. A notable temperature increase is observed from the mid-21st century towards its end across these locations. The urban heat island effect is evident in the higher temperatures recorded at P5 and P6. Despite being in downtown Chicago, P8 has a lower average temperature due to the cooling breezes from Lake Michigan and experiences the least temperature variability, thanks to the significant thermal mass of the lake. P1, being less influenced by urban heat generation, exhibits the lowest average temperature among the four.

Figure 4 shows the annual energy demands of the prototype building at the selected locations, where the marker represents the average, and the shaded area indicates the range from the 10th to the 90th percentiles across all years. There is a gradual increase in cooling energy demand throughout the 21st century across all locations, accompanied by a decrease in heating energy demand. Interestingly, the total energy demand does not show any clear changing trend. For some locations, such as P10 and P11, the TMY3 weather data aligns well with the average of the reanalysis data. However, at other locations, there are some discrepancies between them.

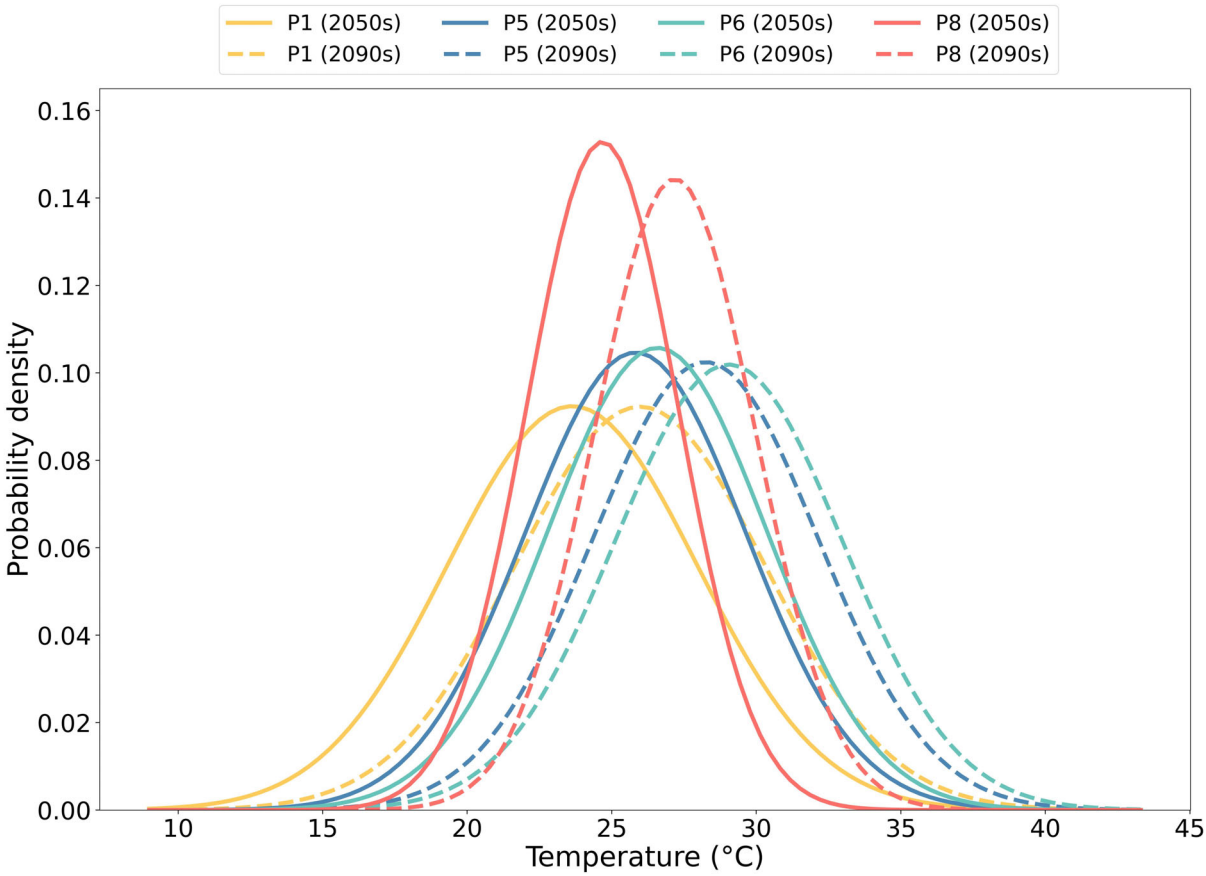

Figure 3: Probability density functions for summer temperatures at four selected locations

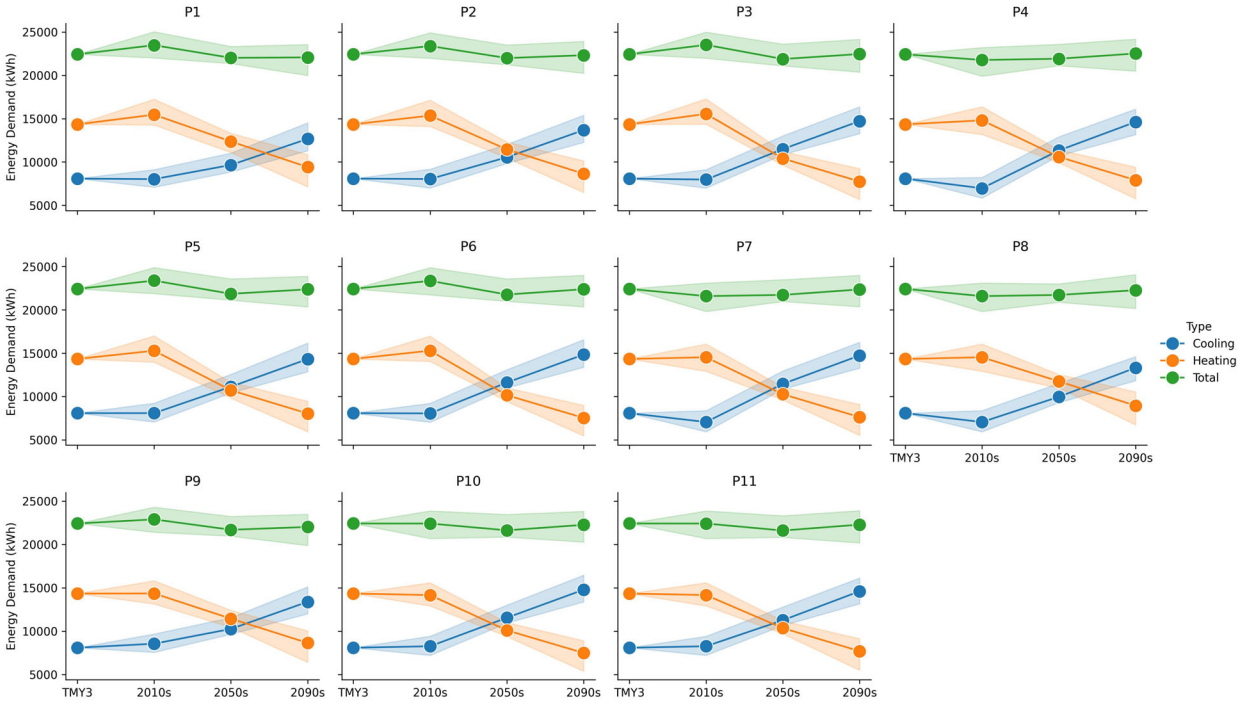

Figure 4: Annual energy demands of the prototype building at the selected locations

Due to the reanalysis data's spatial resolution of ½° × ⅝° (latitude/longitude) being considerably coarser than that of the Argonne Future Weather Dataset, its ability to capture urban-scale microclimates is limited. To avoid inconsistency in comparing weather data of different resolutions, TMY3 weather data is employed as the common baseline for all locations to assess changes in energy demands. Figure 5 illustrates the changes in cooling energy demand for the prototype building over different time periods at the selected locations, with bubble sizes representing the cooling energy demands and their colors indicating the percentage change in cooling energy demand relative to the baseline. Notably, inland urban locations such as P6, P7, and P10 experience the most pronounced increases in cooling energy demand by the 2090s, with surges up to 81%, attributed mainly to the urban heat island effect. Urban areas close to Lake Michigan, especially P8, exhibit smaller increases in cooling energy demand thanks to the lake's mitigating effect. The rise in cooling energy demands diminishes progressively from the city center to suburban and rural areas, with P1 showing the least increase by the 2090s, at 54%.

The changes in heating energy demand for the prototype building over different time periods at the selected locations is illustrated in Figure 6. Similar to cooling energy demand, inland urban locations see the most significant decreases in heating energy demand by the 2090s, reaching up to a 46% reduction. This pattern is less pronounced in lakeshore locations. P1, situated in a rural setting, records the smallest decrease in heating energy demand, with suburban areas showing reductions that fall between those of P1 and the urban locations.

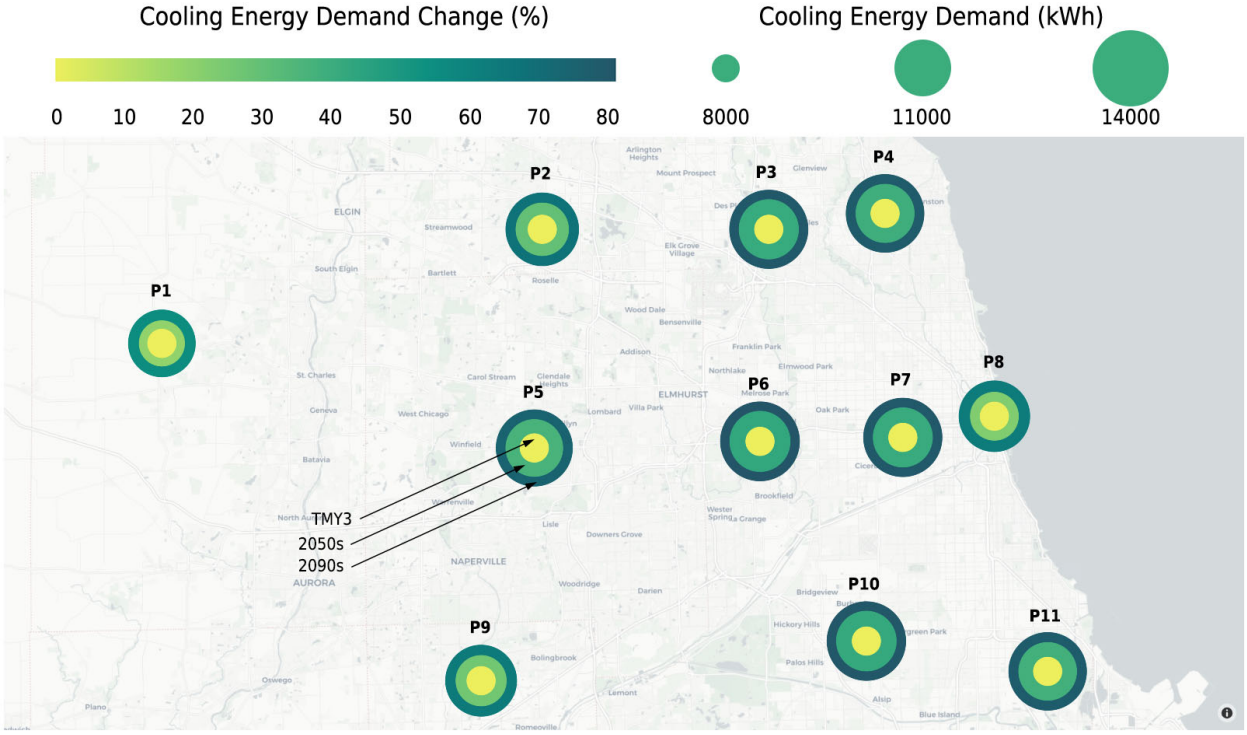

Figure 5: Cooling energy demand change for the prototype building over different time periods at the selected locations

4. CONCLUSIONS

In this paper, we present a concise overview of the methodology used to create future weather data, covering aspects such as emissions scenarios, general circulation models, downscaling techniques, and the various types of future weather data. Additionally, we introduce a dynamically downscaled future weather dataset developed by Argonne National Laboratory. This dataset provides chronological weather data for the periods 2045–2054 and 2085–2094. It features extensive coverage across most of North America and a high spatial resolution of 12 km. Through a case study centered on the Chicago Metropolitan Area, we illustrate the dataset's capability to accurately depict urban microclimates. The results reveal that the Argonne Future Weather Dataset effectively captures the urban heat island effect and the mitigating effects of Lake Michigan.

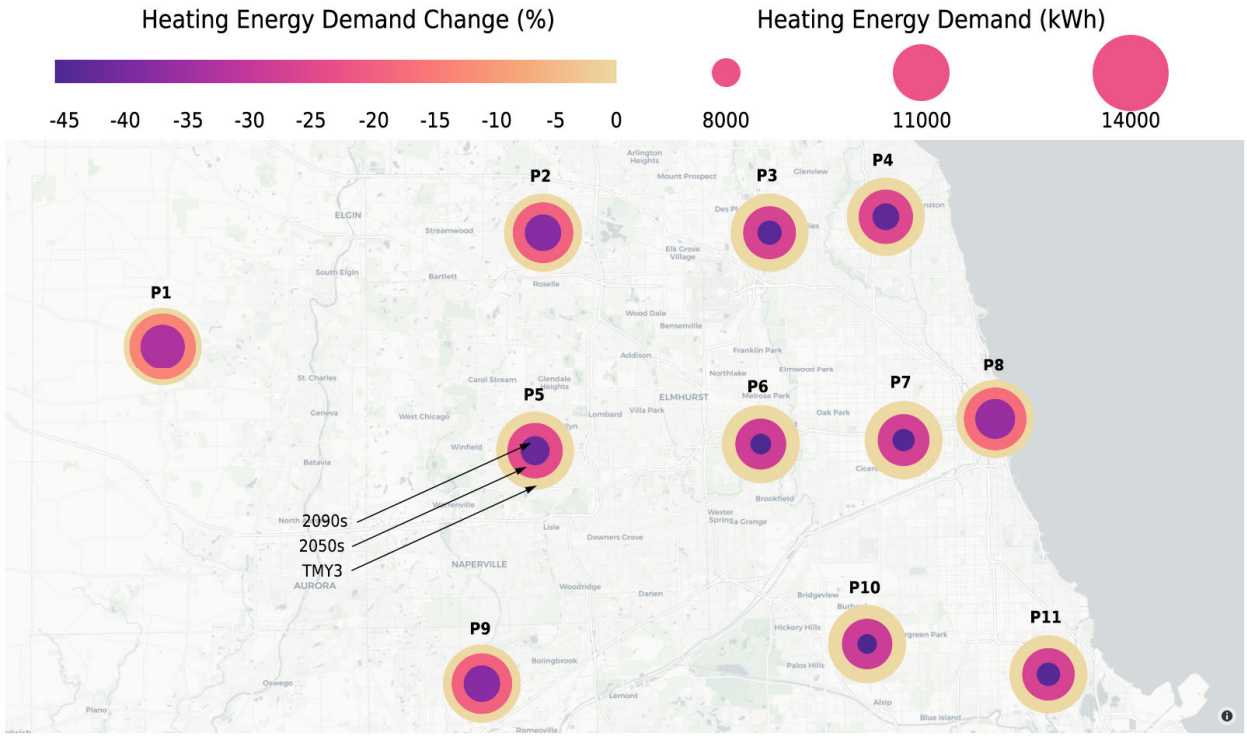

Figure 6: Heating energy demand change for the prototype building over different time periods at the selected locations

REFERENCES

Baniassadi, A., Heusinger, J., & Sailor, D. J. (2018). Energy efficiency vs resiliency to extreme heat and power outages: The role of evolving building energy codes. *Building and Environment*, *139*, 86–94.

Bass, Brett, New, Joshua, Rastogi, Deeksha, & Kao, Shih-Chieh. (2022). *Future Typical Meteorological Year (fTMY) US Weather Files for Building Simulation* (1.0) [dataset]. Zenodo.

Belcher, S. E., Hacker, J. N., & Powell, D. S. (2005). Constructing design weather data for future climates. *Building Services Engineering Research and Technology*, *26*(1), 49–61.

Clark, G., & Allen, C. (1978). The Estimation of Atmospheric Radiation for Clear and Cloudy Skies. *Proceedings 2nd National Passive Solar Conference (AS/ISES)*, 675–678.

Coumou, D., & Rahmstorf, S. (2012). A decade of weather extremes. *Nature Climate Change*, *2*(7), 491–496.

Eames, M. (2016). An update of the UK's design summer years: Probabilistic design summer years for enhanced overheating risk analysis in building design. *Building Services Engineering Research and Technology*, *37*(5), 503–522.

Eames, M., Kershaw, T., & Coley, D. (2011). On the creation of future probabilistic design weather years from UKCP09. *Building Services Engineering Research and Technology*, *32*(2), 127–142.

Ekström, M., Grose, M. R., & Whetton, P. H. (2015). An appraisal of downscaling methods used in climate change research. *WIREs Climate Change*, *6*(3), 301–319.

Feser, F., Rockel, B., von Storch, H., Winterfeldt, J., & Zahn, M. (2011). Regional Climate Models Add Value to Global Model Data: A Review and Selected Examples. *Bulletin of the American Meteorological Society*, *92*(9), 1181–1192.

Flato, G. M. (2011). Earth system models: An overview. *WIREs Climate Change*, *2*(6), 783–800.

Gent, P. R., Danabasoglu, G., Donner, L. J., Holland, M. M., Hunke, E. C., Jayne, S. R., Lawrence, D. M., Neale, R. B., Rasch, P. J., Vertenstein, M., Worley, P. H., Yang, Z.-L., & Zhang, M. (2011). The Community Climate System Model Version 4. *Journal of Climate*, *24*(19), 4973–4991.

Giorgi, F. (2008). Regionalization of climate change information for impact assessment and adaptation. *WMO Bulletin*, *57*(2).

Giorgi, F., & Bates, G. T. (1989). The Climatological Skill of a Regional Model over Complex Terrain. *Monthly Weather Review*, *117*(11), 2325–2347.

Giorgi, F., & Mearns, L. O. (1991). Approaches to the simulation of regional climate change: A review. *Reviews of Geophysics*, *29*(2), 191.

Hannah, L. (2022). The Climate System and Climate Change. In *Climate Change Biology* (pp. 13–50). Elsevier. https://linkinghub.elsevier.com/retrieve/pii/B9780081029756000029

Herrera, M., Natarajan, S., Coley, D. A., Kershaw, T., Ramallo-González, A. P., Eames, M., Fosas, D., & Wood, M. (2017a). A review of current and future weather data for building simulation. *Building Services Engineering Research and Technology*, *38*(5), 602–627.

Herrera, M., Natarajan, S., Coley, D. A., Kershaw, T., Ramallo-González, A. P., Eames, M., Fosas, D., & Wood, M. (2017b). A review of current and future weather data for building simulation. *Building Services Engineering Research and Technology*, 014362441770593.

Ineichen, P. (2008). A broadband simplified version of the Solis clear sky model. *Solar Energy*, *82*(8), 758–762.

Intergovernmental Panel on Climate Change. (2021). *Climate Change 2021: The Physical Science Basis. Contribution of Working Group I to the Sixth Assessment Report of the Intergovernmental Panel on Climate Change* (1st ed.). Cambridge University Press. https://www.cambridge.org/core/product/identifier/9781009157896/type/book

Jentsch, M. F., Bahaj, A. S., & James, P. A. B. (2008). Climate change future proofing of buildings—Generation and assessment of building simulation weather files. *Energy and Buildings*, *40*(12), 2148–2168.

Kyselý, J., & Dubrovský, M. (2005). Simulation of extreme temperature events by a stochastic weather generator: Effects of interdiurnal and interannual variability reproduction. *International Journal of Climatology*, *25*(2), 251–269.

Meehl, G. A., Covey, C., Delworth, T., Latif, M., McAvaney, B., Mitchell, J. F. B., Stouffer, R. J., & Taylor, K. E. (2007). THE WCRP CMIP3 Multimodel Dataset: A New Era in Climate Change Research. *Bulletin of the American Meteorological Society*, *88*(9), 1383–1394.

Meehl, G. A., & Tebaldi, C. (2004). More Intense, More Frequent, and Longer Lasting Heat Waves in the 21st Century. *Science*, *305*(5686), 994–997.

Moss, R. H., Edmonds, J. A., Hibbard, K. A., Manning, M. R., Rose, S. K., van Vuuren, D. P., Carter, T. R., Emori, S., Kainuma, M., Kram, T., Meehl, G. A., Mitchell, J. F. B., Nakicenovic, N., Riahi, K., Smith, S. J., Stouffer, R. J., Thomson, A. M., Weyant, J. P., & Wilbanks, T. J. (2010). The next generation of scenarios for climate change research and assessment. *Nature*, *463*(7282), 747–756.

NASA Langley Research Center. (2023). *NASA POWER | Prediction Of Worldwide Energy Resources*. https://power.larc.nasa.gov/

New, M., Lopez, A., Dessai, S., & Wilby, R. (2007). Challenges in using probabilistic climate change information for impact assessments: An example from the water sector. *Philosophical Transactions of the Royal Society A: Mathematical, Physical and Engineering Sciences*, *365*(1857), 2117–2131.

Nik, V. M. (2016). Making energy simulation easier for future climate – Synthesizing typical and extreme weather data sets out of regional climate models (RCMs). *Applied Energy*, *177*, 204–226.

O'Neill, B. C., Carter, T. R., Ebi, K., Harrison, P. A., Kemp-Benedict, E., Kok, K., Kriegler, E., Preston, B. L., Riahi, K., Sillmann, J., van Ruijven, B. J., van Vuuren, D., Carlisle, D., Conde, C., Fuglestvedt, J., Green, C., Hasegawa, T., Leininger, J., Monteith, S., & Pichs-Madruga, R. (2020). Achievements and needs for the climate change scenario framework. *Nature Climate Change*, *10*(12), 1074–1084.

Pacific Northwest National Laboratory. (2013, July 11). *Residential Prototype Building Models*. U.S. Department of Energy. https://www.energycodes.gov/development/residential/iecc_models

Perez, R., Ineichen, P., Maxwell, E., Seals, R., & Zelenka, A. (1992). Dynamic Global-to-Direct Irradiance Conversion Models. *ASHRAE Transactions*, *98*(1), 354–369.

Powers, J. G., Klemp, J. B., Skamarock, W. C., Davis, C. A., Dudhia, J., Gill, D. O., Coen, J. L., Gochis, D. J., Ahmadov, R., Peckham, S. E., Grell, G. A., Michalakes, J., Trahan, S., Benjamin, S. G., Alexander, C. R., Dimego, G. J., Wang, W., Schwartz, C. S., Romine, G. S., … Duda, M. G. (2017). The Weather Research and Forecasting Model: Overview, System Efforts, and Future Directions. *Bulletin of the American Meteorological Society*, *98*(8), 1717–1737.

Qian, B., Yu, T., Zhang, C., Heiselberg, P., Lei, B., & Yang, L. (2023). A method of determining typical meteorological year for evaluating overheating performance of passive buildings. *Building Simulation*, *16*(4), 511–526.

Riahi, K., van Vuuren, D. P., Kriegler, E., Edmonds, J., O'Neill, B. C., Fujimori, S., Bauer, N., Calvin, K., Dellink, R., Fricko, O., Lutz, W., Popp, A., Cuaresma, J. C., Kc, S., Leimbach, M., Jiang, L., Kram, T., Rao, S.,

Emmerling, J., … Tavoni, M. (2017). The Shared Socioeconomic Pathways and their energy, land use, and greenhouse gas emissions implications: An overview. *Global Environmental Change*, *42*, 153–168.
Taylor, K. E., Stouffer, R. J., & Meehl, G. A. (2012). An Overview of CMIP5 and the Experiment Design. *Bulletin of the American Meteorological Society*, *93*(4), 485–498.
US Census Bureau. (2022, August 22). *Public Use Microdata Areas (PUMAs)*. Census.Gov. https://www.census.gov/programs-surveys/geography/guidance/geo-areas/pumas.html
Van Aalst, M. K. (2006). The impacts of climate change on the risk of natural disasters. *Disasters*, *30*(1), 5–18.
van Vuuren, D. P., Edmonds, J., Kainuma, M., Riahi, K., Thomson, A., Hibbard, K., Hurtt, G. C., Kram, T., Krey, V., Lamarque, J.-F., Masui, T., Meinshausen, M., Nakicenovic, N., Smith, S. J., & Rose, S. K. (2011). The representative concentration pathways: An overview. *Climatic Change*, *109*(1–2), 5–31.
van Vuuren, D. P., Kriegler, E., O'Neill, B. C., Ebi, K. L., Riahi, K., Carter, T. R., Edmonds, J., Hallegatte, S., Kram, T., Mathur, R., & Winkler, H. (2014). A new scenario framework for Climate Change Research: Scenario matrix architecture. *Climatic Change*, *122*(3), 373–386.
Vidal, J.-P., & Wade, S. (2008). A framework for developing high-resolution multi-model climate projections: 21st century scenarios for the UK. *International Journal of Climatology*, *28*(7), 843–858.
Villa, D. L., Schostek, T., Govertsen, K., & Macmillan, M. (2023). A stochastic model of future extreme temperature events for infrastructure analysis. *Environmental Modelling & Software*, *163*, 105663.
Walton, G. N. (1983). *Thermal Analysis Research Program Reference Manual* (NBSSIR 83-2655). National Bureau of Standards.
Wang, J., Liu, Z., Foster, I., Chang, W., Kettimuthu, R., & Kotamarthi, V. R. (2021). Fast and accurate learned multiresolution dynamical downscaling for precipitation. *Geoscientific Model Development*, *14*(10), 6355–6372.
Watkins, R., Levermore, G., & Parkinson, J. (2011). Constructing a future weather file for use in building simulation using UKCP09 projections. *Building Services Engineering Research and Technology*, *32*(3), 293–299.
Wilks, D. S., & Wilby, R. L. (1999). The weather generation game: A review of stochastic weather models. *Progress in Physical Geography: Earth and Environment*, *23*(3), 329–357.
Yang, Z.-L. (2015). Foreword to the special issue: Regional earth system modeling. *Climatic Change*, *129*(3–4), 365–368.
Zeng, Z., Zhang, W., Sun, K., Wei, M., & Hong, T. (2022). Investigation of pre-cooling as a recommended measure to improve residential buildings' thermal resilience during heat waves. *Building and Environment*, *210*, 108694.

ACKNOWLEDGEMENT

This work was supported by the U.S. Department of Energy under Contract No. DE-AC02-06CH11357.